Determination of the Magnetic Axes of Cobalt(II) and Nickel(II) Azurins from ^{1}H NMR Data: Influence of the Metal and Axial Ligands on the Origin of Magnetic Anisotropy in Blue Copper Proteins†

Antonio Donaire,*,‡ Jesús Salgado,§ and José-María Moratal||

Centro de Estudios Universitarios "San Pablo", Universitat de Valencia, Montcada, Valencia, Spain, Gorlaeus Laboratories, Leiden Institute of Chemistry, Leiden University, Einsteinweg 55, P.O. Box 9502, 2300RA Leiden, The Netherlands, and Departamento de Química Inorgánica, Universitat de Valencia, Dr. Moliner, 50, 46100 Burjassot, Valencia, Spain

Received August 11, 1997; Revised Manuscript Received April 1, 1998

ABSTRACT: The orientation and the axial, $\Delta\chi_{ax}$, and rhombic, $\Delta\chi_{rh}$, components of the magnetic susceptibility tensor anisotropy for the cobalt(II) and nickel(II) derivatives of azurin from *Pseudomonas aeruginosa* have been determined from ^{1}H NMR data. For both derivatives, the axial geometry of the system determines the orientation of the χ-tensor, whose *z*-axis forms an angle of 18.6 and 20.1 degrees with the Cu−OGly45 axial bond in the cobalt(II) and nickel(II) derivatives, respectively. For protons close to this axis, large negative pseudocontact shifts are observed, while those close to the NNS plane of the equatorial ligands experience lower and positive pseudocontact shifts for the same distance. Dipolar shifts are larger in the cobalt derivative, not only because of the larger spin number but also due to its intrinsically higher anisotropy. The contact contribution to the hyperfine shifts for the coordinated residues has been evaluated and analyzed in terms of unpaired spin delocalization mechanisms and geometry considerations. The results are extended to other blue copper proteins whose cobalt derivatives have been studied by ^{1}H NMR. The electronic structure and its implications in the redox properties of the native copper proteins are also commented.

The knowledge of the electronic structure of proteins that participate in the electron-transfer chains of biological processes is the first necessary step toward understanding the mechanisms involving them. How the geometry imposed by the protein and to what extent the metal itself modulates the thermodynamic and kinetic properties of such processes are of great interest. With this goal in mind, a large number of techniques and theoretical studies have been applied to a great variety of electron-transfer proteins (for recent reviews, see refs *1*−*5*). Of these techniques, NMR is one of the most powerful because of its ability to determine solution structures, to determine dynamic and electronic properties, and in particular to explore the structure of the metal active site in this type of proteins (*6*−*9*). NMR, as applied to paramagnetic systems, has proven to be crucial due to the intrinsic information that hyperfine shifted signals and relaxation data contain (*10*−*13*). This has been extensively shown in native paramagnetic systems, mainly in low-spin ferric heme proteins (*14*−*21*) but also in ferredoxins (*22*−*27*), high potential iron-sulfur proteins, HiPIPs (*28*), and cytochrome-oxidase (*29*−*31*). In cases where the native system was not appropriate for the application of this technique [i.e., diamagnetic systems, such as Zn-enzymes, or proteins containing paramagnetic ions with slow electronic relaxation, such as blue copper proteins (BCP's, hereafter)], metal substitution has been able to exploit the advantages of paramagnetic NMR. This has been the case for the substitution of Zn(II) and Cu(II) by cobalt(II) ($S = 3/2$) or nickel ($S = 1$) ions (*11*, *32*, *33*).

In a paramagnetic system, the hyperfine shift of an NMR signal is the sum of two contributions. The first, called contact or Fermi contribution, is due to the existence of unpaired spin delocalization on the resonating nucleus, which is transmitted through bonds and becomes undetectable a few chemical bonds away from the metal. The second arises from the dipolar or "through-space" interaction between the electron and the nuclear spin magnetic moments and is called pseudocontact or dipolar contribution. Both give independent and complementary information on the electronic structure of the metal ion and on the role of the geometry and nature of the ligands in the electronic structure. Thus, it is necessary to separate the two contributions in order to obtain the information that they contain. The dipolar shift is due to the magnetic anisotropy of the system, which

† This work has been supported with financial aid from the DGICYT-Ministerio de Educación y Ciencia, Spain (PB94-0989).

* Author to whom correspondence should be addressed at Departamento de Química Inorgánica, Universitat de Valencia, Dr. Moliner, 50, 46100 Burjassot, Valencia, Spain. Phone: 34 6 386 45 97. Fax: 34 6 386 43 22. E-mail: donaire@uv.es.

‡ Centro de Estudios Universitarios "San Pablo", Universitat de Valencia.

§ Gorlaeus Laboratories, Leiden Institute of Chemistry.

|| Departamento de Química Inorgánica. Universitat de Valencia.

[1] Abbreviations: NMR, nuclear magnetic resonance; BCP's, blue copper proteins; EPR, electron paramagnetic resonance; TOCSY, total correlation spectroscopy; NOESY, nuclear Overhauser effect spectroscopy; Az, azurin; CoAz, cobalt(II) azurin; NiAz, nickel(II) azurin; St, stellacyanin; Am, amicyanin; DQF-COSY, double quantum filter correlation spectroscopy; ZFS, zero-field splitting; PDB, protein data bank.

S0006-2960(97)01974-0 CCC: $15.00
Published on Web 05/22/1998

originates from a nonzero orbital contribution to the magnetic moment. If the unpaired electron is localized on the metal nucleus (i.e., by assuming the metal-centered point-dipole approximation (*13*, *34*)), the relationship between the dipolar shift and the magnetic susceptibility tensor anisotropy is defined in eq 1 (*10*, *13*):

$$\delta_{pc} = \frac{1}{12\pi r^3}\left[\Delta\chi_{ax}(3\cos^2\theta - 1) + \frac{3}{2}\Delta\chi_{rh}\sin^2\theta\cos^2\phi\right] \quad (1)$$

where r, θ, and ϕ are the spherical polar coordinates of a proton relative to the principal coordinates of the χ tensor. The axial, $\Delta\chi_{ax}$, and rhombic, $\Delta\chi_{rh}$, magnetic susceptibility anisotropy values are given by:

$$\Delta\chi_{ax} = \chi_{zz} - \frac{1}{2}(\chi_{xx} + \chi_{yy}) \quad (2)$$

and

$$\Delta\chi_{rh} = \chi_{xx} - \chi_{yy} \quad (3)$$

In turn, χ_{xx}, χ_{yy}, and χ_{zz} are the magnitudes of the principal components of the magnetic susceptibility tensor. They can be obtained from the low temperature (4 K) g values if only the ground-state multiplet is populated in the absence of zero-field splitting (ZFS), by the expression

$$\chi_{kk} = \frac{\mu_0\mu_B{}^2 S(S+1)}{3kT} g_{kk}{}^2 \quad (4)$$

Here, μ_B is the Bohr magneton, μ_0 is the permeability of vacuum, k is the Boltzmann constant, T is the absolute temperature, and g_{kk} presents the principal axes (g_{xx}, g_{yy}, and g_{zz}) of the g-tensor.

Equation 1 applies in the magnetic coordinate system in which the magnetic susceptibility tensor, χ, is diagonal. If a sufficient number of specific assignments of protons belonging to noncoordinated residues (i.e., without contact contribution) is obtained and a structural model of the system is available, the orientation of the axes of the magnetic susceptibility tensor anisotropy with respect to this structural model as well as the axial, $\Delta\chi_{ax}$, and equatorial, $\Delta\chi_{rh}$, components of the tensor can be determined. This has been successfully performed in low-spin Fe(III) cytochromes (*17*, *35*−*37*). In some cases, the knowledge of the relative orientation of the magnetic susceptibility tensor has allowed the explanation of the influence of the surrounding ligands on the structural features of the ferric ions in heme proteins. In other systems, the structural information provided by the knowledge of the magnetic susceptibility tensor components and its orientation (see eq 1) has been used as constraints to refine the solution structure of some low-spin iron(III) cytochromes (*38*−*41*). Axial and rhombic magnetic susceptibility anisotropy values obtained by this procedure have also been reported for proteins in which the native Zn(II) ion has been substituted by Co(II). This is the case of the adducts formed by Co(II) human carbonic anhydrase II with perchlorate, nitrate, and thiocyanate (*42*, *43*) and of Cu(I)-Co(II) superoxide dismutase (*44*). There are several studies performed on nickel metallo-substituted proteins by applying ^{1}H NMR spectroscopy in the literature (*45*−*47*); however, the orientation of the magnetic susceptibility tensor has not been reported for any of them.

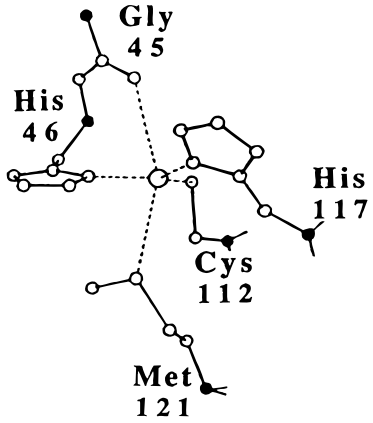

FIGURE 1: Active site of azurin, showing the ligands coordinated to the metal ion.

Once the pseudocontact shifts are known, the contact contribution to the chemical shifts of protons belonging to residues coordinated to the metal ion can be calculated. The dipolar contribution is obtained by using the metal-centered point-dipole approximation (eq 1), and thus the contact contribution determined by this method contains ligand-centered pseudocontact effects (*13*, *34*). In any case, from the calculated contact contribution, the mechanism of spin delocalization onto the ligands and its influence on the interaction with the metal ion can be obtained. Moreover, the comparison of different metal derivatives of the same system can shed light on the nature of the orbitals containing the unpaired electrons. Additionally, information on the relationships between the electronic structure and the redox properties of the protein can be also deduced.

Azurin from *Pseudomonas aeruginosa* is a relatively small protein (127 amino acids), with a blue, type 1, copper active center. The protein is thought to shuttle electrons from the cytochrome *bc1* to nitrite reductase when the bacterium grows in anaerobic conditions (*48*). Azurin is a very well structurally characterized protein; the X-ray structures of the native protein at two different pH values, and in the oxidized and reduced states as well as the structures of several mutants are available (*49*−*54*). The copper ion presents a distorted trigonal bipyramidal geometry where three equatorial donor atoms (Cys112Sγ, His46Nδ1, and His117Nδ1, NNS) are strongly bonded, and the axial ligands (Met121Sδ and Gly45CO) are weakly bonded (Figure 1). The axial methionine has been proposed to govern, to some extent, the electronic and redox properties of azurin and similar blue copper proteins such as plastocyanin, stellacyanin, or amicyanin (*55*−*58*). In these other blue copper proteins there is no axial peptide carbonyl to the metal, and the copper−SδMet121 (or equivalent residue in other BCP's) distance is shorter than in azurin. On the other hand, the orientation of the g-tensor in the Cu(II) azurin has been obtained from electron spin echo (ESE) detected EPR at W-band on a single crystal (*59*). It has been concluded that the g-tensor orientation is governed by the axial geometry of the ligands, as the xy-plane is approximately coplanar with the NNS plane. Thus, knowing to what extent this and other features of the molecular architecture of the metal binding site are controlled by the metal itself or by the protein structure is

decisive. Studying the electronic structure of metallo-substituted derivatives of azurin should help to shed light onto questions such as these.

The cobalt(II) and nickel(II) derivatives of azurins (CoAz and NiAz, hereafter) have been extensively studied by us, not only by NMR (*60*−*64*) but also by EPR in the case of CoAz and by magnetic susceptibility measurements for NiAz (*65*). We have also solved the crystal structure of the nickel derivative (*66*). Very recently, the crystal structure of the cobalt derivative has also been solved (*67*). In addition, an extensive assignment of the hyperfine shifted ^{1}H NMR signals for the cobalt derivative has been performed (*60*, *68*).

We present here the determination of the magnetic susceptibility tensor for cobalt(II) and nickel(II) azurins. The contact and pseudocontact contributions for these proteins have been analyzed, and the features of the active site decisive for the electronic structure of both cobalt(II) and nickel(II) derivatives and the native copper(II) protein are discussed. The role of the metal ion is discussed as well. The results are extended to other blue copper proteins studied by paramagnetic NMR methodology. Finally, implications on the redox properties are also commented.

MATERIALS AND METHODS

Sample Preparation. Azurin from *Pseudomonas aeruginosa* was obtained and purified as previously described (*69*). The nickel(II) derivative was prepared according to a previously published procedure (*62*). Samples used in NMR experiments were typically 2−5 mM, phosphate buffer 50 mM, D_2O 10%, pH 7.5. The temperature ranged from 10 to 40 °C.

NMR Experiments. All NMR experiments were performed on a Unity 400 Varian spectrometer. DQF-COSY spectra (*70*, *71*) were collected at 20 and 40 °C in H_2O over spectral windows of 5400 × 5400 Hz using 1024 × 512 complex data points in t_1 and t_2 dimensions, 128 scans each. The recycle time was 800 ms. H_2O signal was suppressed by presaturation during the relaxation delay. NOESY experiments (*72*) were performed at 10, 20, 30, and 40 °C using presaturation during the relaxation delay and the mixing time. These mixing times ranged from 25 to 200 ms. Clean-TOCSY experiments (*73*, *74*), using MLEV-17 (*75*) as spin lock pulse sequence were collected. Soft 90° pulses of 23 μs were applied. The cycle mixing sequence typically had a duration from 20 ms (for paramagnetic experiments) to 90 ms (for diamagnetic experiments). The other parameters were analogous to those used in the DQF-COSY experiments. For all 2D experiments, the quadrature detection in the t_1 dimension was achieved by employing the hypercomplex method (*76*).

Data were processed using the VNMR1 Varian software on a Sun Sparc 5 work station. For DQF-COSY experiments data points were multiplied by a sine square function, zero-filled to 2048 × 1024 points and Fourier transformed. TOCSY and NOESY experiments were multiplied by a cosine square function shifted 45°, zero-filled to 2048 × 1024 points and Fourier transformed. For NOESY and TOCSY experiments with short mixing times, a line broadening of 3 Hz prior to Fourier transformation was also applied. In these cases, the data points were not zero-filled. All chemical shifts were referenced to 2,2-dimethyl-2-silapentane-5-sulfonate, DSS, through the solvent signal.

Magnetic Susceptibility Tensor. In a paramagnetic system, the observed chemical shift for each proton is the sum of a diamagnetic and a paramagnetic contribution:

$$\delta_{obs} = \delta_{dia} + \delta_{para} \quad (5)$$

where δ_{dia} is the chemical shift of the proton in absence of unpaired spin electron(s). The chemical shift due to the existence of unpaired electron density, δ_{para}, is, in turn, given by the expression:

$$\delta_{para} = \delta_{dip} + \delta_{con} \quad (6)$$

where δ_{dip} represents the "through-space" or pseudocontact contribution and δ_{con} the "through-bonds" or contact contribution. This last factor rapidly decreases with the number of bonds between the observed proton and the paramagnetic metal ion, and so it is negligible for protons that do not belong to residues directly coordinated to the metal ion. It follows that for these protons δ_{para} is equal to δ_{dip}, and hence equal to the difference between the observed, δ_{obs}, and the diamagnetic, δ_{dia}, chemical shift.

The determination of the orientation of the magnetic susceptibility tensor and its axial, $\Delta\chi_{ax}$, and rhombic, $\Delta\chi_{rh}$, anisotropy components was obtained from a fit to five parameters between the observed dipolar shifts ($\delta_{obs} - \delta_{dia}$ for protons of noncoordinated residues) and the calculated dipolar shifts (obtained from eq 1). We have used the previous assignments on the diamagnetic Cu(I)Az (*77*) as the δ_{dia} values of eq 5. The fit was performed with the program FANTASIA (*39*), provided by Professor Bertini (University of Florence, Italy). The method of minimization and the algorithm are described elsewhere (*39*). The X-ray structures of Cu(II) azurin at pH 5.5 (*51*) (pdb4azu.ent coordinates in the Protein Data Bank) and nickel(II) azurin from *P. aeruginosa* (*66*) were used as structural models for the calculation of the dipolar contributions of protons from the cobalt(II) and the nickel(II) derivatives, respectively (very recently, the CoAz crystal structure has been solved (*67*), although its atom coordinates are still not deposited in the PDB). In both cases, the reference system for the Cartesian axes was defined as follows: the cobalt (or nickel) ion was taken as the center, the *x*-axis was defined by the Cu−SγCys112 bond, the *xy*-plane was that formed by the metal ion, the Cys112Sγ and the His46Nδ1 atoms and the *z*-axis was defined as the vectorial product of the vectors connecting these last two atoms with the metal ion, the positive sign pointing toward the Met121Sδ atom.

RESULTS AND DISCUSSION

NMR Experiments. The ^{1}H NMR spectrum of Ni(II)Az derivative at pH 7.5 (40 °C, phosphate 20 mM) is shown in Figure 2A. The dipolar shifts used in the determination of the magnetic susceptibility tensor in the nickel derivative were obtained either from our previous assignments (*62*) (as in the case of Met13, Phe15, and Trp48 protons) or from the 2D experiments described in the Materials and Methods. These assignments are given in Supporting Information. As the aim of the present study was to have a sufficient number of restrictions to obtain a reliable magnetic susceptibility tensor but not the complete assignment of the NiAz signals, the method followed for the assignment of specific spin

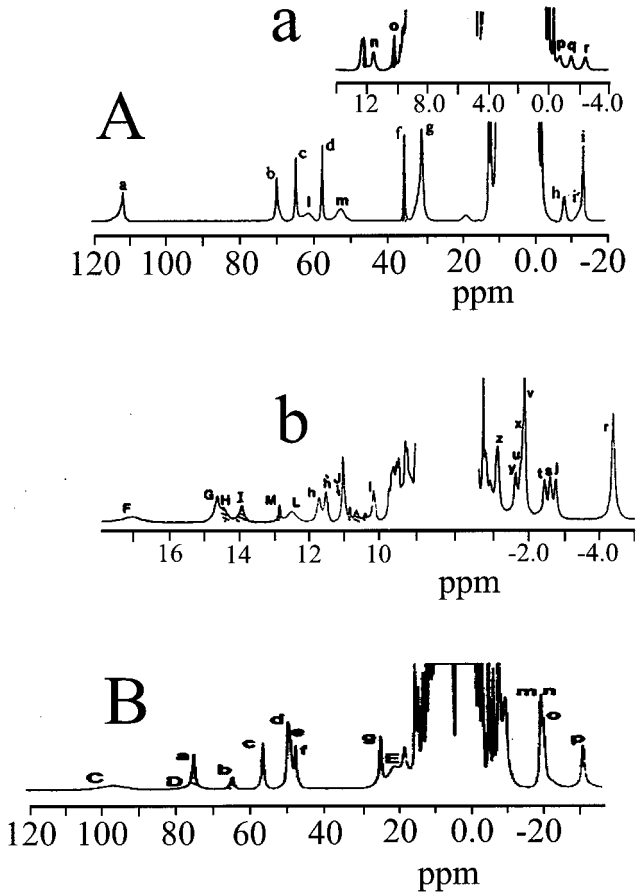

FIGURE 2: ^{1}H NMR spectrum of (A) NiAz from *P. aeruginosa* in H_2O, phosphate 20 mM, pH 7.6, 40 °C; (B) CoAz from *P. aeruginosa* in H_2O, phosphate 20 mM, pH 7.5, 37 °C. In (*a*) and (*b*) expansions of the pseudo-diamagnetic regions of spectra A and B, respectively, are shown.

systems was not the conventional one used for diamagnetic systems. To accelerate the process, for protons relatively further (>8 Å) from the metal ion, we used the previous assignment in the diamagnetic, Cu(I), form (*77*) together with the dipolar connectivities expected from the X-ray structure. The magnetic anisotropy of NiAz is small (see below). This is reflected by the low degree of dispersion in the pseudo-diamagnetic region of the ^{1}H NMR spectrum (see Figure 2a). Thus, the chemical shifts for NiAz resonances do not differ in a large magnitude from those assigned in Cu(I)Az (see Supporting Information) and hence this method is reliable. We have assigned 240 protons, 82 of them placed less than 15 Å from the paramagnetic center, i.e., displaying sizable dipolar shifts (the pseudocontact shift for a proton at 15 Å from the metal ion in the optimum orientation can be as large as −0.3 ppm, see below).

In Figure 2B, the ^{1}H NMR spectrum of Co(II)Az derivative at pH 7.5 (37 °C, phosphate 20 mM) is displayed. As observed, the region of this spectrum corresponding to signals with only dipolar shift contribution is relative large (−8 to 23 ppm, Figure 2b). This indicates a greater degree of anisotropy than in the NiAz derivative. For the CoAz derivative, the previous proton assignment have been used (*60*).

Determination of the Magnetic Susceptibility Tensors. (a) Cobalt Azurin. In Figure 3A, the calculated versus the experimental dipolar shifts for the 109 protons used to obtain the magnetic susceptibility tensor anisotropy components are shown. Of these 109 protons, 103 are at less than 15 Å from the metal ion and hence sizable dipolar shifts are expected. These values together with the assignment of each signal are reported in Supporting Information. As observed, for most of the protons, the fit is quite good, with a small value for the linear regression coefficient (0.97) between the experimental and calculated dipolar shifts (see Figure 3A). Met13γ protons (22.6 ppm, downfield shifted) and Leu86 side-chain protons (up to −8.6 ppm, upfield shifted) exhibit the largest dipolar shifts. For these resonances the predicted and observed values are in very good agreement. Other protons whose predicted pseudocontact chemical shifts nicely agree with the previous assignments are those belonging to residues Lys41, Asn42, Met44, Trp48, Val49, Leu68, Ile87, Phe110, Pro115, Gly116, Ser118, and Leu120. All of these are less than 13 Å from the cobalt ion and show pseudocontact contributions that vary from 11.2 ppm (for Met44Hγ2 proton) to −5.6 ppm (for Lys41Hα proton). These data confirm the previous assignments and the reliability of the obtained tensor components. However, some protons, like Hα, Hβ1, and Hβ2 from Met13 and HN and Hα from Asn47, experience dipolar shifts that deviate from the calculated values. These data points were excluded from the calculations. The justification for which we present below. Met13 Hα and Hβ protons are very close to the metal ion (at distances of 4.8, 5.5, and 7.0 Å, respectively) and in such an orientation that the magnitude of the tensor is relatively large (see below), so small conformational (structural) differences between the CoAz solution structure and the Cu(II)Az crystal structure could cause large variations in the chemical shifts. However, it is important to notice that, even if the calculations of the magnetic susceptibility tensor are performed without the contribution of the Met13Hγ protons, the difference between the calculated and observed pseudocontact shifts for these two methylene protons is very small. The amide proton of Asn47 is hydrogen bonded to Cys112Sγ, and consequently both the HN and the Hα protons are expected to have contact contribution to their isotropic shifts (*78*−*81*) as is indeed observed (see below). We have also to keep in mind that formation or disruption of a hydrogen bond considerably changes the chemical shift both in diamagnetic and in paramagnetic derivatives.

The values of the magnetic susceptibility anisotropy components for the CoAz derivative are given in Table 1. The angles of the main axes with respect to the axial and equatorial bonds are also given in this table and displayed in Figure 4A. The $\Delta\chi_{ax}$ and $\Delta\chi_{rh}$ values for CoAz are large compared with NiAz and CuAz (see Table 1). This is due both to the $S = 3/2$ value and to the large magnetic anisotropy. Sizable magnetic anisotropy in six-coordinated high-spin cobalt(II) complexes has been attributed to spin−orbit coupling and low symmetry components (*34*, *82*). For highly symmetric tetrahedral $S = 3/2$ cobalt(II) complexes, magnetic anisotropy only arises from zero-field splitting effects. In our intermediate situation, with five coordination for the cobalt ion, both mechanisms are expected to be operative, although to a lesser extent than for six-coordinated cobalt(II).

The effective *g* values (although not the orientation of the *g*-tensor) have been obtained from EPR measurements at 5 K (*65*). In that EPR study, it was concluded that the mean

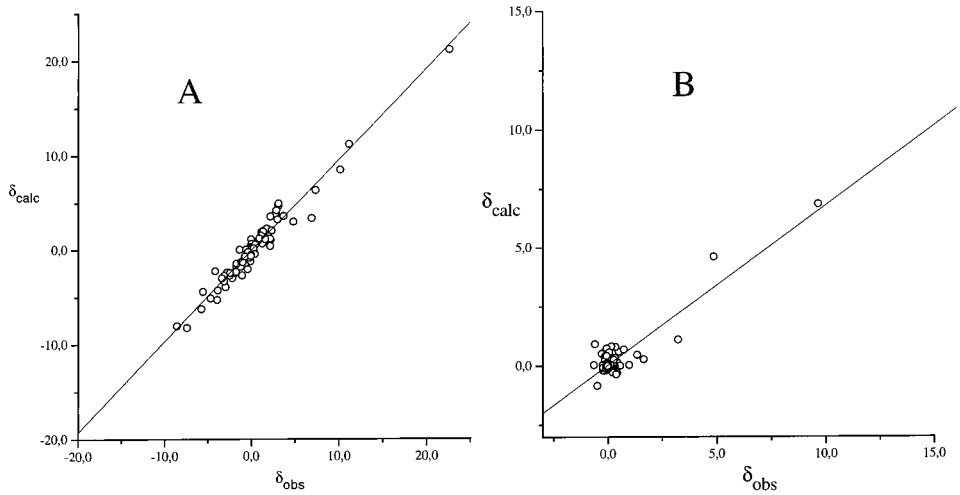

FIGURE 3: Plot of the experimental versus calculated dipolar shifts in (A) CoAz and (B) NiAz.

Table 1: Angles (in degrees) of the Main Axes of the Magnetic Susceptibility Tensor with Respect to the Bonds between the Metal Ion and the Coordinated Atoms for the Cobalt(II) and Nickel(II) Azurins from *P. aeruginosa*[a]

	Gly45CO	Met121Sδ	Cys112Sγ	His46 Nδ1	His117Nδ1
			Co(II)Az		
χ_{xx}	$73 \pm 4°$	$92 \pm 4°$	$96 \pm 4°$	$37 \pm 4°$	$139 \pm 4°$
χ_{yy}	$83 \pm 5°$	$83 \pm 5°$	$174 \pm 5°$	$54 \pm 5°$	$51 \pm 5°$
χ_{zz}	$19 \pm 4°$	$159 \pm 4°$	$91 \pm 4°$	$95 \pm 4°$	$81 \pm 4°$
$\Delta\chi_{ax}$ ($m^3 \times 10^{32}$)	-6.8 ± 0.3				
$\Delta\chi_{rh}$ ($m^3 \times 10^{32}$)	2.8 ± 0.1				
			Ni(II)Az		
χ_{xx}	$76 \pm 11°$	$126 \pm 11°$	$87 \pm 11°$	$147 \pm 11°$	$50 \pm 11°$
χ_{yy}	$76 \pm 12°$	$112 \pm 12°$	$22 \pm 12°$	$112 \pm 12°$	$141 \pm 12°$
χ_{zz}	$20 \pm 10°$	$136 \pm 10°$	$112 \pm 10°$	$67 \pm 10°$	$100 \pm 10°$
$\Delta\chi_{ax}$ ($m^3 \times 10^{32}$)	-2.0 ± 0.4				
$\Delta\chi_{rh}$ ($m^3 \times 10^{32}$)	-0.9 ± 0.2				
			Cu(II)Az		
g_{xx}	$77.2 \pm 1.4°$	$79.0 \pm 1.7°$	$112.8 \pm 1.6°$	$19.3 \pm 2.5°$	$124.5 \pm 2.1°$
g_{yy}	$101.9 \pm 1.7°$	$99.2 \pm 1.2°$	$24.1 \pm 1.7°$	$109.1 \pm 2.5°$	$145.3 \pm 2.1°$
g_{zz}	$162.3 \pm 1.8°$	$14.5 \pm 1.2°$	$97.1 \pm 1.5°$	$90.1 \pm 2.7°$	$88.6 \pm 3.1°$
$\Delta\chi_{ax}$ ($m^3 \times 10^{32}$)[b]	0.634				
$\Delta\chi_{rh}$ ($m^3 \times 10^{32}$)[b]	-0.047				

[a] Calculated magnetic susceptibility anisotropy components are given as well. For comparison, the orientation of the g_{xx}, g_{yy}, and g_{zz} axes of the *g*-tensor in the oxidized Cu(II) protein (obtained from ref *59*) are also given. [b] For the native protein the $\Delta\chi_{ax}$ and $\Delta\chi_{rh}$ values have been obtained by applying eq 4 and assuming that only the ground state is populated (low-temperature approximation).

g value of ≈2.3 was consistent with a second-order spin−orbit coupling and an orbitally nondegenerate ground state. It was concluded, as well, that the best geometry describing the metal site was a highly distorted tetrahedral geometry with a trigonal coordination, where one of the axial ligands is moving away from the cobalt center. This picture is also consistent with our results if the observed magnetic susceptibility tensor anisotropy values arise mainly, if not exclusively, from low symmetry components. In the tetrahedral adduct of cobalt(II) bovine carbonic anhydrase with cyanate (*83*) chemical shifts as large as +20 and −5 ppm have been determined for protons belonging to noncoordinated residues. In this tetrahedral complex the magnetic anisotropy arises only from ZFS effects. Thus, a similar situation probably occurs in CoAz.

As a result of the large magnetic anisotropy present in the CoAz derivative, an ample chemical shift dispersion in the proximity of the diamagnetic part of the ^{1}H NMR spectrum is observed (see Figure 2b). The *xy*-plane of the χ-tensor is nearly coplanar with the plane of the NNS equatorial donor atoms (the angle between the director vectors of these two planes is 19.2°), while the *z*-axis points toward the Gly45 carbonyl oxygen, forming an angle of 18.6° with respect to the Cu−OGly45 bond. This orientation of the magnetic susceptibility tensor produces large negative dipolar contributions at residues oriented toward the axial ligands, while those located close to the NNS plane experience smaller and positive dipolar shifts. Figure 5 displays the calculated pseudocontact chemical shift that a hypothetical proton oriented in each of the directions of the five metal−ligand bonds would experience as a function of the distance to the metal ion. As observed, protons of the axial ligands have negative (upfield) dipolar shifts, while those of the equatorial ligands have positive (downfield) and smaller pseudocontact contributions to their chemical shifts. Finally, it is also interesting to notice that the *y*-axis is nearly coincident with the Co−SγCys112 bond (only 5.7° of deviation). This orientation is different from the one found in Cu(II) azurin (*59*), as well as in the Ni(II) derivative (see below).

(b) Nickel Azurin. The assignment of 240 protons to noncoordinated residues in NiAz has allowed us to obtain the

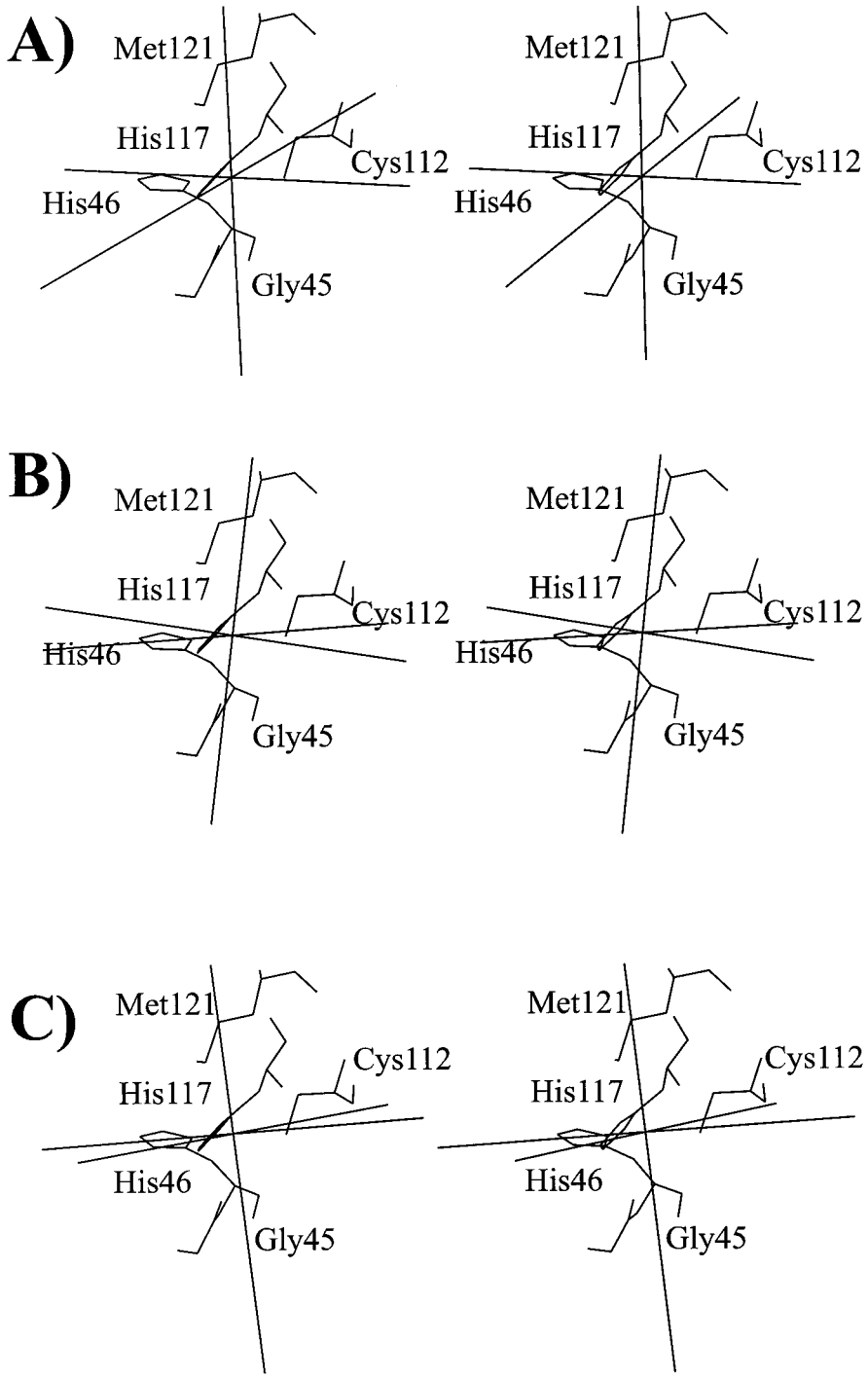

FIGURE 4: Stereoview representation of the principal axes of the magnetic susceptibility tensor with respect to the metal−ligand bonds for (A) Co(II)Az derivative (B) Ni(II)Az derivative. The orientation of the *g*-tensor for the oxidized native, Cu(II)Az (obtained from ref *59*), is displayed in Figure C.

components and orientation of the magnetic susceptibility tensor in this derivative. The experimental versus the calculated dipolar shifts for these signals are plotted in Figure 3B. In Table 1, the values of the axial and equatorial components together with the angles between the main axes and the Ni-donor atoms are given. A good agreement between the experimental and calculated values is observed for protons belonging to residues Met13 and Phe114, which are the only assigned residues placed less than 6 Å from the metal. Thus, the calculated tensor components are strongly influenced by the value of the dipolar shifts of these signals. The other resonances used in the calculations belong to residues farther than 6 Å from the metal ion, and their contribution to the fit is less than that of the Met13 and Phe114 protons. It was not possible to assign other residues within a 6 Å sphere of the paramagnetic center as all of these resonances fall in the diamagnetic envelope and, therefore, overlap problems arise (see Figure 2a). This is a consequence and, at the same time, the first evidence of the low magnetic anisotropy present in the NiAz derivative. Due to the overlap problems, the linear regression fit between the experimental and observed dipolar shifts is not as good as for the cobalt derivative. However, the values of the tensor obtained by excluding Met13 and Phe114 protons differ only

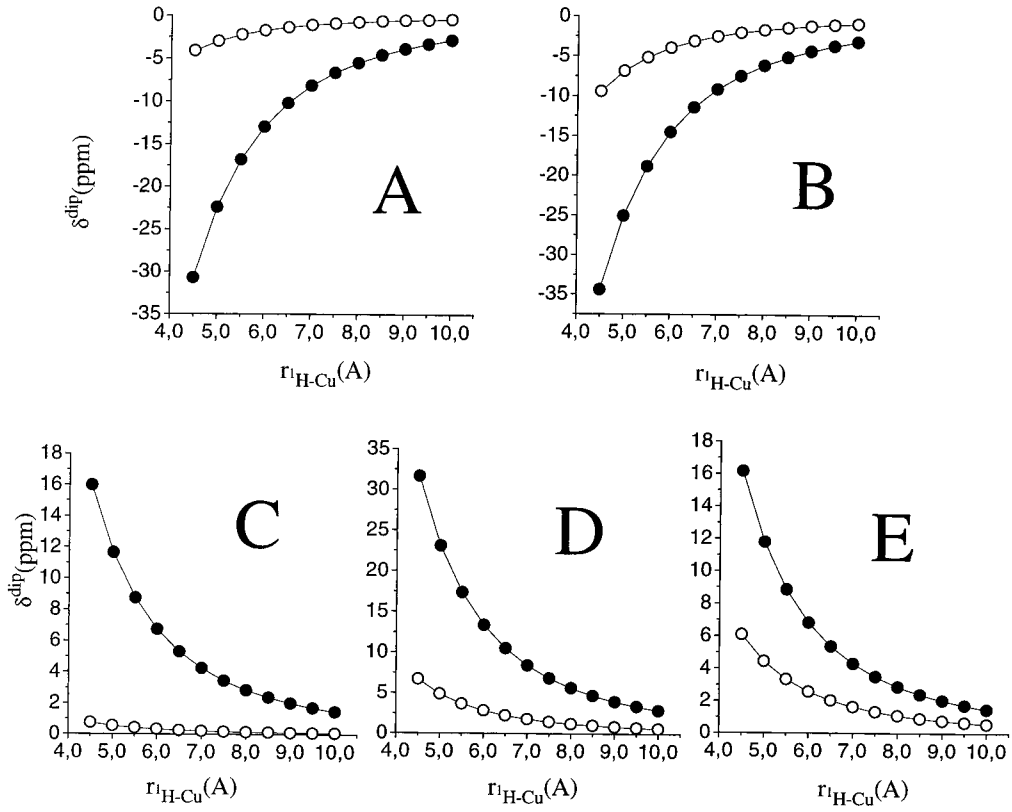

FIGURE 5: Calculated pseudocontact contributions to the chemical shifts as a function of the distance for hypothetical protons placed along the straight lines defined by the following bonds (A) Cu−SδMet121, (B) Cu−OCGly45, (C) Cu−SγCys112, (D) Cu−Nδ1His46, and (E) Cu−Nδ1His117. Solid and open circles refer to CoAz and NiAz, respectively.

in the magnitude of the $\Delta\chi_{ax}$ and $\Delta\chi_{rh}$ components (-1.97×10^{-32} and -0.92×10^{-32} m^3 including these residues, Table 1, versus -0.99×10^{-32} and -0.54×10^{-32} m^3, without them, respectively), but not in the orientation of the tensor. So, the following results, with regard to the magnetic moment orientation, are completely reliable. We believe that the increment in the magnitude of the calculated magnetic moment when the calculations include protons of Met13 and Phe114 (i.e., those closest to the metal ion) could be due to small differences between the solution and the crystal structure for these two amino acids. In any case, the values of $\Delta\chi_{ax}$ and $\Delta\chi_{rh}$ shown in Table 1 for NiAz represent the upper limit of the axial and rhombic magnetic susceptibility anisotropy components.

The values of Table 1 for NiAz indicate, first, a relatively small magnetic susceptibility tensor anisotropy values and, second, an orientation of the *xy*-plane almost coplanar with the NNS plane (see Figure 4B). The first feature suggests the existence of a ground state that is orbitally nondegenerate (or close to it) and low zero-field splitting effects. In octahedral Ni(II) complexes, these two characteristics are expected, while for tetrahedral nickel(II) a higher degree of magnetic anisotropy is found (*34*, *82*). From magnetic susceptibility measurements in NiAz between 5 and 130 K, an axial zero-field splitting parameter, D_S, of 17.7 cm^{-1} was obtained, which was explained by assuming a distorted five-coordinate trigonal geometry for the metal ion (*65*). The NiAz crystal structure (*66*) shows that the Met121Sδ atom is weakly bound to the metal ion, with a bond length of 3.30 Å. Our present results clearly show that Met121 is coordinated to the metal ion, since the large isotropic shift for Met121Hγ signal can only be explained by a large contact contribution. Tetrahedral nickel(II) complexes have a triplet ground state that causes large e magnetic anisotropy (*34*, *82*). The relatively small magnetic susceptibility tensor anisotropy values, as well as the minimal dispersion of the paramagnetically shifted resonances of the ^{1}H NMR spectrum observed for this derivative (Figure 2a) can be explained by the presence of a five-coordinated nickel(II) center.

With regard to the orientation of the tensor, the *z*-axis in the nickel derivative tensor (Table 1, Figure 4B) is oriented, as in the cobalt derivative, almost perpendicular to the NNS plane of the metal-coordinated atoms. As in the case of the cobalt derivative, the axial geometry determines the orientation of the tensor and, analogously, such orientation produces positive (downfield) dipolar contribution to the protons oriented close to the equatorial plane and larger and negative contribution to protons close to the axial ligands (see Figure 5).

Comparison of the Magnetic Susceptibility Tensors of Co, Ni, and Cu Azurins. The orientation of the *g*-tensor of the native azurin in the oxidized Cu(II) protein has been determined by ESE-detected EPR (*59*). For comparison, the components of the magnetic susceptibility tensor anisotropy of Cu(II)Az obtained by applying eq 4 (and, hence, by assuming that only the ground state is populated) are also given in Table 1. The orientation of the *g*-tensor with respect to the metal−ligand bonds is also displayed in Figure 4C. The *z*-axis is inclined 162° with respect to the Cu−OCGly45 bond, that is the same orientation as in the nickel derivative although in opposite sense. The *y*-axis is shifted 24.1° degrees with respect to the Cu−SγCys112 bond, which is also very close to the value obtained in the nickel derivative (22.4°, see Table 1). Thus, the replacement of Cu(II) by

Table 2: Contact and Dipolar Contributions for the Hyperfine Shifts of the Protons of the Coordinated Residues for Cobalt and Nickel Azurins from *P. aeruginosa*[a]

		chemical shifts (ppm)						
		CuAz	CoAz			NiAz		
amino acid	proton[b]	δ_{dia}	δ_{obs}	δ_{dip}	δ_{con}	δ_{obs}	δ_{dip}	δ_{con}
Gly45	HN	5.9	6.8	−9.80	10.7	7.9	−5.4	7.4
	Hα1	4.1	47.8	−10.53	54.2	69.5	−6.5	65.4
	Hα2	3.2	−29.4	−26.71	−5.9	−14.1	−5.9	−11.4
His46	HN	8.2	−9.1	−11.22	−6.1	2.6	−6.0	0.4
	Hα							
	Hβ1	3.3	16.0	7.08	5.6			
	Hβ2	2.4	20.3	16.69	1.3			
	Hε1	6.9	97.0	85.69	4.4	61.2	17.0	37.3
	Hδ2	5.6	50.6	7.75	37.3	57.2	−0.3	51.9
	Hε2	11.5	74.9	16.56	46.9	35.0	2.0	21.5
Cys112[b]	Hβ1	3.4	232	5.38	223.2	187.3	1.1	182.8
	Hβ2	2.9	285	−5.27	287.4	232.6	−9.8	239.5
His117	HN	8.8	14.6	2.56	3.2	10.1	−1.3	2.6
	Hα	4.8	5.5	1.92	−1.3			
	Hβ1							
	Hβ2							
	Hε1	6.8	75.0	23.25	45.0	52.6	9.7	36.1
	Hδ2	6.9	56.4	7.18	42.3	64.3	1.6	55.9
	Hε2	11.6	65.8	7.47	46.8	51.5	3.7	36.2
Met121	HN	9.1	1.7	−5.52	−1.8	7.9	−3.2	2.1
	Hα	4.3	−3.2	−9.93	2.5	4.3	5.2	−2.0
	Hβ1	1.7	−18.9	−25.93	5.3	−2.5	−8.1	3.9
	Hβ2	2.2	−18.5	−26.85	6.1	−1.6	−4.4	0.6
	Hγ1	1.4	45.3	−19.53	64.4	111.3	−2.7	112.5
	Hγ2	1.4	−19.1	−20.22	−0.3	0.6	−4.9	4.04
	$CH_{3}\epsilon$	−0.1	−7.3	−31.21	24.0	30.3	−0.1	30.4
Asn47	HN	10.6	7.0	30.1	−33.6			
	Hα	4.7	15.4	5.36	5.3			

[a] Asn47 backbone protons, which also show contact shifts (see text), are given as well. Diamagnetic shift values (δ_{dia}) have been taken from ref *77*. [b] Cys112 Hβ protons have been stereospecifically assigned for NiAz, but not for CoAz. In this table, the proton with the largest chemical shift in NiAz (Hβ2 proton) is assumed to be the same in the CoAz derivative.

Ni(II) in azurin results in only a small change in the orientation of the magnetic susceptibility tensor. This implies that the electronic structure of the metal is governed by the nature and the geometry of the ligands, imposed, in turn, by the protein architecture. When Ni(II) is replaced by Co(II) the *z*-axis of the tensor remains oriented toward the axial ligands (Table 1, Figure 4A). Again, this confirms that the nature and the geometry of the ligands govern the electronic structure of the metal.

The ratios of the anisotropy values of the magnetic susceptibility tensor (obtained from Table 1)

$$\frac{(\Delta\chi_{ax})_{Co}}{(\Delta\chi_{ax})_{Ni}} = 3.4$$

and

$$\frac{(\Delta\chi_{eq})_{Co}}{(\Delta\chi_{eq})_{Ni}} = 3.1$$

are larger than 15/8, the value expected if only the difference in the spin number of both metal ions is taken into account in eq 4. This means that a larger magnetic anisotropy is present in the cobalt derivative, which is consistent with the larger ZFS effects observed for this derivative.

From the discussion above, it is clear that the magnitude of the $\Delta\chi_{ax}$ and $\Delta\chi_{rh}$ components depends on characteristics of the metal ion, such as the spin state and the nature of the ground state and low-energy excited levels. In contrast, the orientation of the main axes of the magnetic susceptibility tensor depends on the geometry of the ligand binding site. Hence, for azurin metallo-derivatives, the metal binding site geometry, and not the metal ion itself, is the principal determinant of the orientation of the magnetic susceptibility moment.

Contact Contribution on the Coordinated Residues. Once the magnetic susceptibility anisotropy values are known, the dipolar contribution of any proton can be calculated. In particular, those belonging to the coordinated residues are of special interest. The resonance assignment of protons belonging to these residues has previously been performed for both cobalt and nickel azurins (*60*−*64*, *68*), thus, the contact contribution can immediately be obtained by applying eq 6. The experimental shifts and the diamagnetic, dipolar, and contact contributions for these protons in both CoAz and NiAz are given in Table 2.

The contact contribution to the chemical shift depends on the unpaired spin density that resides on a given proton. Two mechanisms have been proposed to account for this spin delocalization (*13*, *34*, *82*). The first mechanism, called direct unpaired spin density transfer, always transmits unpaired spin density of the same sign. The second, called spin-polarization, involves a mechanism where the sign of the spin density can change between consecutive nuclei. Here, we comment on the relative importance of these two factors on the hyperfine shifts of each ligand proton and its

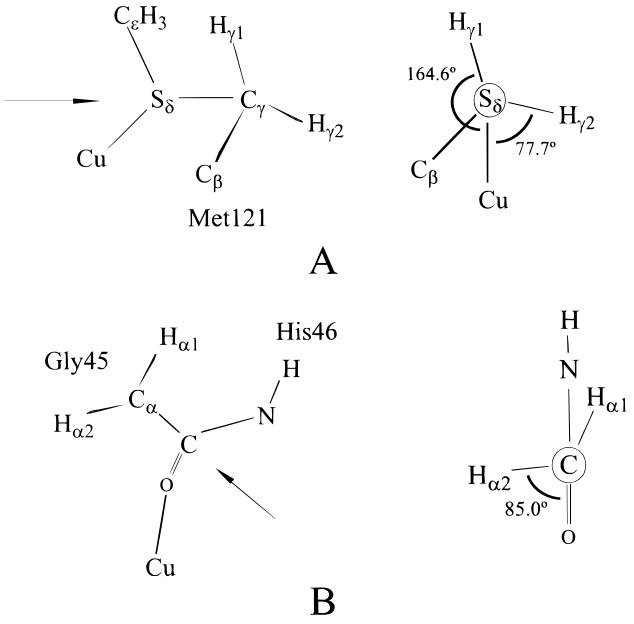

FIGURE 6: Schematic representation of the dihedral angles involving the metal and (A) Met121Sδ, Cγ and Hγ atoms; (B) Gly45 backbone atoms and the His46 amide proton. Figures on the left indicate the position of the amino acids with respect to the metal ion. Figures on the right represent the projection of the figures on the left along the Met121Sδ−Cγ bond for Figure A and the Gly45Cα−CO bond for figure B. The arrows indicate these bonds and the atom that is above in the projections.

relationship with the electronic structure of the metal ion. As the contact chemical shifts given in Table 2 contain ligand-centered pseudocontact contributions, that are not evaluated with this methodology, the following discussion on the contact contribution is only partially quantitative. For the nickel(II) derivative the errors in the magnetic susceptibility anisotropy values are not as low as for the cobalt(II) azurin, and hence the conclusion has to be accepted in a more qualitative form.

(a) Axial Ligands. The two Met121Hγ methylene protons show a very different pattern with regard to their hyperfine shifts in both CoAz and NiAz derivatives (see Table 2). In both derivatives, stereospecific assignments have been performed on the basis of the observed NOE connectivities and the X-ray crystal structure (*60*). For the case of Met121Hγ2 proton the contact contribution is negligible (−0.3 and 4.0 ppm for CoAz and NiAz, respectively) and, since the Hγ2 proton is close to the *z*-axis of the magnetic susceptibility tensor, its dipolar contribution is negative. As a result, Met121Hγ2 proton appears upfield shifted in both derivatives. On the contrary, the Met121Hγ1 proton feels a strong contact contribution (64.4 and 112.5 ppm for the cobalt and nickel azurins, respectively). It follows that for these two protons geometric factors are crucial in determining their hyperfine shifts. The contact contribution is related to the M−Sδ-Cγ-Hγ dihedral angles (Figure 6A), through a Karplus-type relationship (*84*):

$$\delta = (\cos^2\theta + a\cos\theta + b)A\rho_s \qquad (7)$$

where *a*, *b*, and *A* are constants, θ is the M−Sδ-Cγ-Hγ dihedral angle and ρ_s the unpaired spin density localized on the sulfur atom. In most cases, *a* and *b* are negligible and the contact shift will simply depend on the square cosine (or square sine, see below) of the dihedral angle θ. If only σ bonds are involved in the spin delocalization, the contact chemical shifts for these protons have to follow the previously indicated square cosine dependence. This has been found for nickel(II) complexes with amine ligands (*85*, *86*). For ferredoxins and HiPIPs, this relationship has been found to depend on the square sine of the equivalent dihedral angle (*27*, *87*−*89*). This is due to the fact that the unpaired spin density mainly resides in a p_z orbital of the sulfur atom, orthogonal to the Fe−S bond, and thus, a π-type spin delocalization is dominant. In Figure 6A, the dihedral angles for both methylene protons are given according to the Cu(II)Az X-ray structure (in the nickel derivative crystal structure, the deviation of these angles with respect to the Cu(II)Az structure is lower than 5°). The Cu−Sδ-Cγ-Hγ dihedral angles are −164.6° and 77.7° for the Hγ1 and the Hγ2 protons, respectively. Due to the existence of dipolar ligand-centered effects, it is not possible to obtain a good quantitative correlation between these dihedral angles and the contact chemical shifts. However, qualitative conclusions can be extracted from the present data. As Met121Hγ2 proton has negligible contact chemical shift and the Cu−Sδ-Cγ-Hγ2 dihedral angle is very close to 90 degrees (in both CoAz and NiAz), the operative spin transfer mechanism in Met121Hγ protons must act through σ bonds. Due to the fact that, in azurin, the Met121Sγ is weakly bound to the metal ion (3.15 and 3.30 Å in copper and nickel azurins, respectively), any overlap between orbitals orthogonal to the σ-bond of the metal ion and the p_z sulfur orbital is negligible. Moreover, the magnetic susceptibility tensor is oriented in this same direction. Therefore, the main, if not the only, contribution to spin delocalization at these two methylene protons must arise from an orbital with an unpaired electron which is oriented directly toward the Met121Sδ atom, i.e., the d_{z^2} orbital. Therefore, in both nickel and cobalt derivatives, an unpaired electron resides in that orbital.

In the case of the other axial ligand, Gly45, a different situation is found. While the Met121Hγ protons are connected to the metal ion through three bonds, Gly45Hα protons are coupled to the metal ion through four bonds, one of which (the C═O bond) has π electron density. In both the cobalt and nickel derivatives, the Gly45Hα1 proton shows large downfield contact contribution. In contrast, Gly45Hα2 proton feels smaller, although still sizable, upfield contact shift (see Table 2). This indicates that, first, geometric factors are determinant for the unpaired spin density residing at these two methylene protons and, second, the spin polarization mechanism is operative since different signs of unpaired spin density are present at both nuclei. Moreover, a negative contact contribution for the Hα2 proton (Table 2) means that for this proton direct spin density transfer is small compared to spin polarization, which is dominant and negative in sign. Negative spin polarization on this proton is possibly due to the alternating sign of the polarization from consecutive atoms. Figure 6B displays the dihedral angle between the O═C−Cα and C−Cα-Hα planes for the two methylene protons according to the CuAz crystal structure (essentially the same angle is found in the NiAz X-ray structure). For the Hα2 proton, this dihedral angle has a value of 85.0 degrees. We cannot discriminate between the magnitude of the spin polarization mechanism and the direct spin transfer for these two protons and, hence, it is

not possible to find quantitatively a Karplus relationship. However, as the total contact contribution is much larger in magnitude for the Hα1 proton than for the Hα2 proton (Table 2), then, if a Karplus relationship applies for these protons, it has to follow a square cosine dependence, i.e., the unpaired spin delocalization is operative through σ bonds.

Another interesting point concerns the chemical shift of the His46 amide proton. This proton shows negative contact contribution in CoAz and negligible in NiAz (see Table 2). The upfield shift of the CoAz derivative has to arise from spin polarization mechanisms, while a zero value for the NiAz derivative can only arise from a cancellation between direct spin transfer (positive) and spin polarization (negative) mechanisms, which would be similar in magnitude. Since the number of bonds from the metal to this proton is the same as in the case of the Gly45 methylene protons (Figure 6B), it follows that polarization alternates in sign in the same way for both set of protons in these two bonds. However, His46HN is in the same plane as the (Gly45)O═C−N(His46) atoms (see Figure 6B). If σ delocalization operates through this peptide bond, large and positive shifts would be observed (as happens for Gly45Hα1, Table 2). On the contrary, this mechanism has to be negligible because such shifts are not observed. It is possible that direct spin density transfer through the peptide bond occurs via π-delocalization mechanisms and, hence, is not operative on the *1s* orbital of the His46HN proton. Another, maybe more plausible, explanation would be that spin polarization mechanisms on the π system of the peptide bond would be large enough in magnitude (negative in sign) to compensate direct (positive) unpaired spin transfer residing on the His46HN proton, transmitted via σ bonds. This could be possible because spin polarization is expected to be larger on π delocalized systems than through σ bonds (*13*, *90*−*92*).

(b) Equatorial Ligands. The discussion of the contact contribution to the hyperfine shifts for protons belonging to equatorial ligands is more complicated than for axial ligands. First, more than one orbital containing unpaired electrons contributes to the hyperfine shifts of these protons. Second, these orbitals have both *x* and *y* components, while the ligand orientation is, in general, not coincident with these axes of the χ-tensor. Third, both σ and π delocalization mechanisms are operative. Finally, geometric factors also hinder the interpretation of the hyperfine shifts. However, several conclusions can be extracted by comparing the data from the cobalt and nickel derivatives in Table 2. The Cys112Hβ protons are located in such an orientation with respect to the magnetic susceptibility tensor that the pseudocontact contribution is negligible, even though these protons are very close to the metal ion. In fact, for both metallo-derivatives, the Cys112Hβ1 proton shows a positive dipolar shift, while its stereo-partner experiences a negative pseudocontact shift (see Table 2). As a consequence of this, the observed chemical shifts are almost exclusively due to contact contribution. The smaller paramagnetic shifts of Cys112Hβ protons in NiAz than in CoAz are a consequence of the contribution of the extra unpaired electron of the cobalt(II) ion. From our present results, it is not possible to determine which mechanisms are involved in transferring unpaired spin density to these two protons, although some insights can be obtained. Asn47HN is hydrogen bonded to Cys112Sγ donor atom and, thus, is two bonds from the metal ion. This proton shows negative spin density due to spin polarization effects. Since the Cys112Hβ protons are three bonds from the metal ion and connected to it through the same sulfur donor, it is probable that spin polarization is of opposite sign than that present in the Asn47 amide proton, i.e., positive. The difference in the shifts of Cys112Hβ methylene protons is attributable to slight differences in the magnitude of the M−Sγ-Cβ-Hβ dihedral angles. These dihedral angles are 65° and −54° for the Hβ1 and Hβ2 protons, respectively. These methylene protons have only been stereospecifically assigned in the nickel derivative. In this case, Cys112 Hβ2 has larger contact contribution than the Hβ1 proton (239.5 ppm vs 182.8 ppm, see Table 2). From these data, it can be deduced that the dihedral angle dependence for the protons of an equatorial ligand depends on the squared cosine rather than the squared sine of the M−Sγ-Cβ-Hβ dihedral angle (a smaller angle for the most shifted proton would correspond with a cosine dependence). It is likely that CoAz displays the same dependency.

Interpretation of the chemical shift of the imidazole ring protons is much more complex than for the Cys112Hβ methylene protons. As shown in Table 2, hyperfine shifts for these protons are mainly due to contact contribution in both metal derivatives. A large number of studies have been analyzed on the mechanisms of transferring unpaired electron density in delocalized π-systems, mainly in iron and nickel complexes with imidazole or other aromatic ligands (*90*, *93*−*97*). Polarization effects, σ and π spin delocalization, and ligand-centered dipolar effects contribute to the observed hyperfine shifts for these systems. From our present work, it is not possible to obtain information on the predominant mechanism that acts in these ligands.

The Asn47HN chemical shift deserves a special comment. This proton is hydrogen bonded to Cys112Sγ and is only 4.1 Å from the metal ion. Thus, it should feel a large dipolar contribution in the cobalt derivative (30.1 ppm, see Table 2). However, the observed chemical shift (6.98 ppm) is even lower than that observed in the diamagnetic protein (see Table 2). It follows that a large and negative contact contribution (−33.6 ppm, see Table 2) has to be operative to account for such an observed chemical shift. A similar, although quantitatively different, situation is found for Asn47Hα proton; however, in this case the contact shift is positive. Consequently, in both cases, contact contribution must be sizable. For the amide proton a negative contact shift means that the spin polarization is greater in magnitude than the direct σ electron density transfer, while for the Hα proton either both mechanisms have the same sign or the polarization effects are less. The existence of hydrogen bond networks in the surroundings of the metal ion(s) has been suggested as one of the factors determining the redox potentials of a number of electron-transfer proteins (*98*−*100*). Since hydrogen bonds perturb the electronic structure of the metal ion(s), and hence their redox potential, the unpaired electron density is also expected to be transferred through hydrogen bonds to these protons. This has been observed by ^{15}N NMR and ENDOR spectroscopies on iron-sulfur proteins (*79*, *81*, *101*−*104*). Our present results confirm that the contact shift is transmitted through hydrogen bonds although less efficiently than through covalent bonds, as is the case of the Cys112Hβ protons.

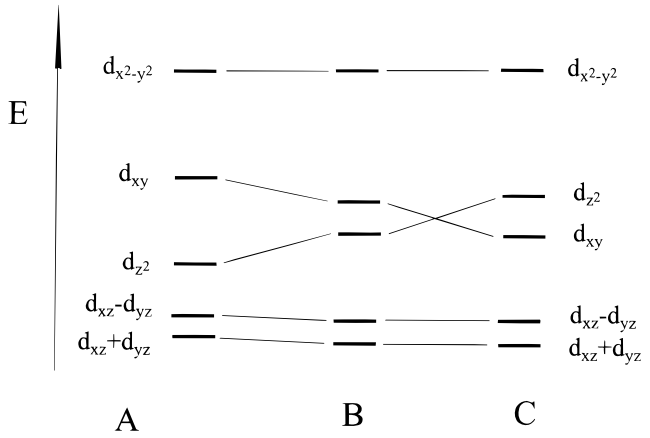

FIGURE 7: Qualitative energy level diagrams for the metal ion in (A) copper (II) plastocyanin, from ref *109*; (B) copper plastocyanin with a shorter distance for the Cu(II)−SδMet92 bond (axial methionine, equivalent to Met121 in azurin, same reference); and (C) nickel and cobalt azurins, with two axial interactions (Gly45CO and Met121Sδ), as proposed in this work.

Electronic Structure of Cobalt and Nickel Azurins. The electronic structure of the copper(II) ion in BCP's is a point of crucial interest for understanding the redox properties of this kind of proteins. Several studies have been applied to the oxidized protein to determine the nature of the orbital where the unpaired electron lies (*3*, *59*, *105*−*108*). In plastocyanin, this electron is, to a first approximation, localized in the $d_{x^2-y^2}$ orbital of the Cu(II) ion (Figure 7A) (*109*). The effects of the axial thioether bond on the energy of *d* orbitals have been analyzed with respect to the bond length (*109*). These results indicate that the d_{z^2} orbital increases and the d_{xy} orbital decreases in energy as the axial methionine sulfur gets closer (Figure 7B). The axial interaction of Gly45CO could have a similar destabilizing effect on the d_{z^2} orbital. As mentioned in the previous section, the unpaired spin density on the Met121Hγ protons arises from spin delocalization via σ bonds. Due to the orientation of the χ-tensor and the long distance of the Ni−SγMet121 bond, this spin delocalization has to be transferred through the d_{z^2} orbital, i.e., this orbital contains an unpaired electron in both NiAz and CoAz. When passing from NiAz to CoAz, the main effect of the additional unpaired electron (in CoAz) is to enlarge the contact shifts of the protons from the equatorial cysteine, but the contact contributions of the protons belonging to the axial ligands (Met121 and Gly45 protons) are not substantially modified. This strongly suggests that, first, the two unpaired electrons of CoAz lie in the same *d* orbitals as the analogous electrons of NiAz, and, second, the third unpaired electron (in the cobalt derivative) essentially lies in an orbital with no *z* component. Thus, the d_{z^2} orbital has greater energy than the d_{xy} orbital in both CoAz and NiAz, and therefore we propose the energy level diagrams displayed in Figure 7C. As the orientation of the *g*-tensor is due to geometric factors and these are essentially retained in the copper(II) protein, we believe that an analogous (at least, qualitatively) energy level diagram applies to the native azurin.

Other Copper Proteins. To our knowledge, the following cobalt derivatives of blue copper proteins (native or mutants) have been studied by ^{1}H NMR: cobalt(II)azurin (*60*, *61*), cobalt(II)C112Dazurin (CoC112DAz) (*68*), cobalt(II)-M121Qazurin (CoM121QAz) (*64*), cobalt(II)amicyanin (CoAm) (*110*), and cobalt(II)stellacyanin (CoSt) (111). Nickel derivatives of the following copper type 1 proteins have been studied by ^{1}H NMR: nickel(II)azurin (*62*−*64*) and nickel(II)M121Qazurin (*62*). Our present results can be extended to all of these systems. Table 3 provides chemical shift data for the proton ligands of these derivatives (for comparison with analogous data in Table 2, azurin derivatives used in Table 3 are those from *Alcaligenes denitrificans*, these values are nearly the same as for azurin from *P. aeruginosa*, and, hence, the discussion applies for both). All cobalt(II) substituted proteins show upfield shifted signals belonging to axial ligands or for protons located close to them. This strongly suggests a similar orientation of the magnetic susceptibility tensor in all these metallo-substituted BCP's. Moreover, the close similarity of the chemical shift patterns for analogous ligands strongly suggests similar contact contributions for equivalent protons. In all the previous works, knowledge of the metal ligands and to what extent they are bound to the metal was a first goal and trends to rationalize the observed hyperfine shifts were described. Now, as both dipolar and contact contributions are known, we can state which protons have contact contribution in these systems and, hence, which are the metal ligands in solution for each protein. In CoM121QAz (*64*), the Gly45Hα signals have small hyperfine shifts (see Table 3). This has been associated with a lack of coordination of this ligand. In fact, the −10.5 ppm for the Gly45Hα2 proton shift in CoM121QAz is easily explained by assuming a similar orientation of the magnetic susceptibility tensor as in CoAz and with only dipolar pseudocontact contribution (the δ_{pc} for Gly45Hα1 and Hα2 in CoAz are −10.5 and −26.7 ppm, see Table 2). In CoSt (where there is a Gln ligand instead of a Met in the same position), an unidentified set of upfield shifted signals between −5 and −30 ppm is present (*111*). We believe that these signals belong to residues close to axial positions because these protons should experience large negative dipolar shifts. It is interesting to notice that, in the NiM121QAz derivative (*62*), the Gly45Hα1 resonates at 28.9 ppm, which cannot be explained by assuming only a dipolar contribution, because in that orientation the pseudocontact contribution is small and negative (−6.5 ppm for NiAz, see Table 2). Hence, Gly45 is at least weakly coordinated in NiM121QAz. This fact indicates that if the donor atom changes, the metal ion can modulate to a small but nonetheless significant degree the geometry of the active site. Thus, although the metal ion is not determinant in defining the architecture of the metal binding site, it can be an important factor if the substituted ligand has very different affinity for the two metal ions.

In Table 4 the estimated contact chemical shift for the most shifted axial ligand protons (Gly45Hα1 and Met121Hγ1 protons) as well as Cys112Hβ protons (or equivalent protons in the several mutants of other BCPs) are given. The contact shifts have been estimated by assuming a similar orientation of the magnetic susceptibility tensor for cobalt and nickel derivatives as in the CoAz and NiAz, respectively, and by assuming similar orientation of these protons. From the observed ^{1}H NMR spectra, the first assumption is, to a first approximation, clearly supported. The second hypothesis must also be correct as it is deduced from the corresponding crystal and solution protein structures (*49*−*53*, *57*, *58*). The contact contribution for these ligand protons in similar

Table 3: Experimental Chemical Shifts of Protons Belonging to Coordinated Residues for the Cobalt(II) and Nickel(II) Derivatives of the Blue Copper Proteins That Have Been Studied by ^{1}H NMR

		Co substituted BCPs					Ni substituted BCPs	
amino acid[a]	proton	azurin[b]	M121QAz[b]	St[c]	C112DAz[d]	Am[e]	azurin[b]	M121QAz[b]
Cys112[f]	Hβ1	222	183	180		280	197	237
	Hβ2	262	224	206		280	238	178
Asp112					44			
					44			
His117	Hϵ1	76	83	86	102		59	49.0
	Hϵ2	64.4	67.4	63.4	52		53.4	54.1
	Hδ2	56.7	56.8	51.4	57		65.7	55.7
His46	Hϵ1	90	125	115	14		59	43.5
	Hϵ2	75.6	73.4	74.4	62		37.5	33.5
	Hδ2	48.9	47.2	45.3	51		60.3	65.1
	Hβ1		−28.6				−14.4	−16.3
	HN				30			
Gly45	Hα1	49.0	5.9		91		63.7	28.9
	Hα2	−26.3	−10.5		13		−13.2	−2.3
	HN				15			
Met121	$CH_3\epsilon$	−5.7				77	43.7	
	Hγ1	39.2				130	101.1	
	Hγ2	−14.7				−17	7.7	
	Hβ1	−15.0				−18	−4.4	
	Hβ2	−15.7				−20	−1.6	
	Hα							
Gln121	Hϵ21		−26.4					−8.9
	Hγ1		46.4	66.2				37.7
	Hγ2		−12.8	−5.8				−8.6
	Hβ1		−22.7	−18.6				2.4
	Hβ2		−15.0					5.2
	Hα		−3.2	−1.1				3.9

[a] Amino acid numbers are referred to *P. aeruginosa* azurin; for stellacyanin from *R. vernicifera*, the equivalent metal ligands are, in the same order as in the table, Cys87, His46, His 92, and Gln97 (the equivalent amino acid to Gly45, i.e., Ala45, is not coordinated); for amicyanin the analogous ligands are Cys112, His54, His96, and Met99. [b] CoAz, CoM121QAz, NiAz, and NiM121QAz from refs *60*, *64*. [c] CoSt from ref *111*. [d] CoC112DAz from ref *68*. [e] CoAm from ref *110*. [f] Except for the NiAz derivative, stereospecific assignment of Cys112 Hβ protons (or equivalent protons in St and Am) have not been performed; they are correlated in this table according to the magnitude of their chemical shifts. For comparison with the observed data in Table 2, azurin derivative values in this table are those corresponding to azurin from *A. denitrificans* (these values are very similar compared to those found in azurin from *P. aeruginosa*, see Table 2).

Table 4: Contact Chemical Shifts for the Most Shifted Protons of the Axial and Cysteine Ligands in Cobalt(II) and Nickel(II) Metallo-substituted BCP's[a]

	contact shift (in ppm)		
metal derivative	Gly45Hα1	Met121Hγ1	Cys112Hβ2
CoAz	54.2	64.4	253
CoM121QAz	13.2	53.7	215
CoSt	not coordinated	73.5	197
CoC112DAz	98.3	not coordinated	
CoAm		137.3	
NiAz	69.5	112.5	224
NiM121QAz	32.2	40.6	223

[a] As indicated in the text, for the proteins not studied in this work the pseudocontact shifts have been assumed to be the same as in CoAz and NiAz, for cobalt and nickel derivatives, respectively. For the St and Am derivatives, the same considerations with respect to the ligands as in Table 3 have been taken. Diamagnetic contribution (negligible in all cases with respect to contact contribution) has been assumed to be the same as in Cu(I)Az (*77*) for equivalent protons, i.e., that given in Table 2. Numbering of residues corresponds to the *P. aeruginosa* azurin sequence.

systems is a good parameter for determining the degree of binding of these ligands to the metal. With regard to Gly45, we can include nickel(II) and cobalt(II) derivatives in the same series since, as mentioned in the previous section, unpaired spin density on this ligand is almost completely due to the direct σ interaction between the carbonyl oxygen and the d_{z^2} metal orbital. With this in mind, the contact chemical shift for Gly45Hα methylene protons would correspond to the bond strength for the M(II)−OCGly45 bond, and follows the rule (see Table 4):

CoC112DAsp > NiAz > CoAz > NiM121QAz > CoM121QAz > CoSt

In fact, in CoC112DAsp, Met121 is not coordinated to the metal ion, while in CoSt the axial coordination is entirely due to this amino acid, as Ala45 (equivalent amino acid in stellacyanin to Gly45 in azurin) is not coordinated at all. Some conclusions arise from this series. First, stellacyanin has the lowest metal ion affinity. In this series, stellacyanin is the only protein that is not an azurin mutant, and, hence, the metal binding site is less similar to the rest of the proteins. Thus, the pocket in the vicinity of the metal ion is the main factor in determining the number of ligands and mode of coordination. Second, when Met121 is replaced by Gln121 (the same ligand as in stellacyanin) in azurin, the metal shows lower affinity for the carbonyl of Gly45. This happens independently of the metal ion. However, for the same protein (wild-type or mutant) nickel(II) shows higher affinity for the carbonyl oxygen. In fact, the contact chemical shifts for Gly45 Hα protons are larger in Ni(II)Az and Ni(II)-M121QAz derivatives than in Co(II)Az and in Co(II)-M121QAz derivatives, respectively (Table 4). Finally, a mutation in one equatorial ligand causes a drastic change in the affinity of the metal for the axial ligands. It is probable that such a large change in the coordination is due to the fact that this equatorial ligand (Cys112) has the greatest interaction with the metal ion. Therefore, any change in the

nature of this amino acid results in acute modification of the metal coordination.

Conversely, the affinity for the axial position corresponding to Met121 in native azurin (Met99 in *Thiobacillus versutus* amicyanin and Gln97 in *Rhus vernicifera* St) can also be determined by the chemical shifts of the protons of this ligand. The nature of the donor atom is different in a Met (thioether sulfur) than in a Gln residue (carbonyl oxygen). Additionally, Met121 Hγ protons are at three bonds from the metal ion (see Figure 6A), while the Gln Hγ protons are at four bonds from the metal ion (the position of these protons is the same as Gly45 Hα protons, see Figure 6B). Hence, the contact chemical shifts for these two methylene protons will depend on these two factors and will vary independently for Met and Gln protons. In this case, two different series according to the amino acid ligand are obtained:

CoAm > NiAz > CoAz > CoC112DAz

CoSt > CoM121QAz > NiM121QAz

This is nearly the opposite as for the Gly45 series (the exception is the NiAz and CoAz relative inequality position). The metal derivatives with higher affinity for the carbonyl of Gly45 show lower affinity for the opposite axial ligand, as expected. These two series also demonstrate the validity of the contact chemical shift as reference for showing the relative affinity of the metal ion for the ligands.

Finally, with regard to the coordination of Cys112, the following ligand affinity series can be determined (Table 4):

CoAm > CoAz > CoM121QAz > CoSt

NiAz $\approx$ NiM121QAz

In this case we have discriminated between cobalt and nickel derivatives because (see previous section) for this ligand contact contribution is different in both metallo-derivatives. The smaller hyperfine shifts of the Cys112Hβ protons in CoM121QAz compared to those of CoAz have been associated with a movement of the metal out of the equatorial plane toward the Gln121 donor atom, that, in turn, reduces the overlap between orbitals of the cobalt and cysteine sulfur (*64*).

The previous discussion suggests that changes from five- to four-coordination in blue copper proteins (such as azurin, stellacyanin, and amicyanin) are governed primarily by the arrangement of the amino acid ligands around the metal ion (i.e., the pocket itself) and the nature of the atom donors in the equatorial (mostly cysteine) position. Changes in the axial ligand(s) and the metal itself are two further factors that modify metal coordination features, but to a lesser extent.

Redox Implications. We have just stated that the nature of the metal has minimal influence on the metal arrangement. Copper(II) is expected to have similar behavior to that already described for nickel(II) and cobalt(II), but here the oxidation state of copper is probably more important than the nature of the metal ion itself. In fact, it has been observed that differences in chemical shifts between copper(I) and copper(II) in plastocyanin are larger than those observed between copper(II) and cadmium(II) derivatives (*112*). In light of this fact, our conclusions may be extended to oxidized blue copper proteins. Greater stabilization of the copper(II) site corresponds to a lower redox potential. So, axial ligand substitutions at the Met121 position in azurin (or equivalent positions in other BCPs) that stabilize copper(II) will produce mutant proteins with a lower redox potential and vice versa. As demonstrated here, this hypothesis can be tested by replacing the native copper ion by cobalt(II) or nickel(II) ions and studying the corresponding derivatives by NMR.

CONCLUSIONS

The present work shows the ability of NMR applied to paramagnetic systems to obtain electronic structure information on a native protein through the use of Co(II) and Ni(II) derivatives.

The calculation of the magnetic susceptibility tensor has enabled us to determine the relative importance of the metal ion and the active site geometry for the orientation of the magnetic axes. The axial nature of the magnetic anisotropy arises from the metal active site architecture, imposed by the protein.

The knowledge of the pseudocontact shifts of protons from the coordinated residues has allowed us to obtain the contact contribution to the hyperfine shifts of these ligand protons. This demonstrates the clear contact bonding interaction in the case of the methionine axial ligand, despite the long bond distance. The contact shifts of the axial ligands (Met121 and Gly45) depend on orientation factors according to a Karplus relationship. The way of binding of the axial Met121 can be related with redox potential of different blue copper proteins. The energy levels of the metal ion *d* orbitals from the native and metallo-substituted azurins are qualitatively comparable.

The analysis and methodology presented in this work can be easily extended to other blue copper proteins.

ACKNOWLEDGMENT

Professor Ivano Bertini from the University of Florence is acknowledged for kindly providing us the FANTASIA program. Dr. Andrea Romagnoli is acknowledged for his extensive and indispensable explanations on practical aspects of the FANTASIA program. Dr. Alejandro J. Vila (University of Rosario, Argentina) is also acknowledged for many helpful discussions.

SUPPORTING INFORMATION AVAILABLE

Two tables with the experimental ($\delta_{obs} - \delta_{dia}$) and expected (according to eq 1) chemical shifts of the assigned protons in NiAz and CoAz (9 pages). Ordering information is given on any current masthead page.

REFERENCES

1. Holm, R. H., Kennepohl, P., and Solomon, E. I. (1996) *Chem. Rev. 96*, 2239−2314.
2. Gray, H. B., and Winkler, J. R. (1996) *Annu. Rev. Biochem. 65*, 537−561.
3. Solomon, E. I., Penfield, K. W., Geweirth, A. A., Lowery, M. D., Shadle, S. E., Guckert, G. A., and LaCroix, L. B. (1996) *Inorg. Chim. Acta 243*, 67−78.
4. Solomon, E. I., Baldwin, M. J., and Lowery, M. D. (1992) *Chem. Rev. 92*, 521−542.
5. Sykes, A. G. (1991) in *Advances in Inorganic Chemistry* (Sykes, A. G., Ed.) pp 377−408, Academic Press, New York.
6. Williams, G., Moore, G. R., Porteous, R., Robinson, M. N., Soffe, N., and Williams, R. J. P. (1985) *J. Mol. Biol. 183*, 409−428.
7. Williams, G., Moore, G. R., and Williams, R. J. P. (1985) *Comments Inorg. Chem. 4*, 55−98.

8. Scheek, R. M., van Gunsteren, W. F., and Kaptein, R. (1989) *Methods Enzymol. 177*, 204−218.
9. Detlefsen, D. J., Thanabal, V., Pecoraro, V. L., and Wagner, G. (1991) *Biochemistry 30*, 9040−9046.
10. La Mar, G. N. and de Ropp, J. S. (1993) in *Biological Magnetic Resonance* (Berliner, L. J., and Reuben, J., Eds.) Vol. 12, pp 1−78, Plenum Press, New York.
11. Bertini, I., Turano, P., and Vila, A. J. (1993) *Chem. Rev. 93*, 2833−2932.
12. La Mar, G. N. (1995) in *NMR of Paramagnetic Macromolecules* (La Mar, G. N., Ed.) NATO ASI Series, Dordrecht, The Netherlands.
13. Bertini, I., and Luchinat, C. (1996) NMR of paramagnetic substances, in *Coordination Chemistry Reviews* (Lever, A. B. P., Ed.) Vol. 150, Elsevier, Amsterdam.
14. Turner, D. L., Salgueiro, C. A., Schenkels, P., LeGall, J., and Xavier, A. V. (1995) *Biochim. Biophys. Acta 1246*, 24−28.
15. Coutinho, I., and Xavier, A. V. (1994) *Methods Enzymol. 243*, 119−140.
16. Palma, P. N., Moura, I., LeGall, J., van Beeumen, J., Wampler, J. E., and Moura, J. J. G. (1994) *Biochemistry 33*, 6394−6407.
17. Clark, K., Dugad, L. B., Bartsch, R. G., Cusanovich, M. A., and La Mar, G. N. (1996) *J. Am. Chem. Soc. 118*, 4654−4664.
18. Chen, Z. G., de Ropp, J. S., Hernandez, G., and La Mar, G. N. (1994) *J. Am. Chem. Soc. 116*, 8772−8783.
19. Turner, D. L. (1995) *Eur. J. Biochem. 227*, 829−837.
20. Banci, L., Bertini, I., Marconi, S., Pierattelli, R., and Sligar, S. G. (1994) *J. Am. Chem. Soc. 116*, 4866−4873.
21. Banci, L., Bertini, I., Bruschi, M., Sompornpisut, P., and Turano, P. (1996) *Proc. Natl. Acad. Sci. U.S.A. 93*, 14396−14400.
22. Calzolai, L., Gorst, C. M., Zhao, Z. H., Teng, Q., Adams, M. W. W., and La Mar, G. N. (1995) *Biochemistry 34*, 11373−11384.
23. Gorst, C. M., Yeh, Y.-H., Teng, Q., Calzolai, L., Zhou, Z.-H., Adams, M. W. W., and La Mar, G. N. (1995) *Biochemistry 34*, 600−610.
24. Donaire, A., Gorst, C. M., Zhou, Z. H., Adams, M. W. W., and La Mar, G. N. (1994) *J. Am. Chem. Soc. 116*, 6841−6849.
25. Aono, S., Bertini, I., Cowan, J. A., Luchinat, C., Rosato, A., and Viezzoli, M. S. (1996) *J. Biol. Inorg. Chem. 1*, 523−528.
26. Bertini, I., Dikiy, A., Luchinat, C., Macinai, R., Viezzoli, M. S., and Vincenzini, M. (1997) *Biochemistry 36*, 3570−3579.
27. Bertini, I., Capozzi, F., Luchinat, C., Piccioli, M., and Vila, A. J. (1994) *J. Am. Chem. Soc. 116*, 651−660.
28. Bertini, I., Donaire, A., Felli, I. C., Luchinat, C., and Rosato, A. (1997) *Inorg. Chem. 36*, 4798−4803.
29. Bertini, I., Bren, K. L., Clemente, A., Fee, J. A., Gray, H. B., Luchinat, C., Malmström, B. G., Richards, J. H., Sanders, D., and Slutter, C. E. (1996) *J. Am. Chem. Soc. 46*, 11658−11659.
30. Dennison, C., Berg, A., de Vries, S., and Canters, G. W. (1996) *FEBS Lett. 394*, 340−344.
31. Murthy, N. N., Karlin, K. D., Bertini, I., and Luchinat, C. (1997) *J. Am. Chem. Soc. 119*, 2156−2162.
32. Donaire, A., Salgado, J., Jimenez, H. R., and Moratal, J. M. (1995) in *Nuclear Magnetic Resonance of Paramagnetic Macromolecules* (La Mar, G. N., Ed.) pp 213−244, Kluwer Academic Publishers, Dordrecht, The Netherlands.
33. Banci, L., and Piccioli, M. (1996) in *Encyclopedia of Magnetic Resonance* (Grant, D. M., and Harris, R. K., Eds.) pp 1365−1373, Wiley, Chichester, U.K.
34. Bertini, I., & Luchinat, C. (1986) in *NMR of paramagnetic molecules in biological systems*, Benjamin/Cummings, Menlo Park, CA.
35. Rajarathnam, K., La Mar, G. N., Chiu, M. L., and Sligar, S. G. (1992) *J. Am. Chem. Soc. 114*, 9048−9058.
36. La Mar, G. N., Chen, Z. G., Vyas, K., and McPherson, A. D. (1995) *J. Am. Chem. Soc. 117*, 411−419.
37. Banci, L., Bertini, I., Pierattelli, R., Tien, M., and Vila, A. J. (1995) *J. Am. Chem. Soc. 117*, 8659−8667.
38. Gochin, M., and Roder, H. (1995) *Bull. Magn. Reson. 17*, 1−4.
39. Banci, L., Bertini, I., Bren, K. L., Cremonini, M. A., Gray, H. B., Luchinat, C., and Turano, P. (1996) *J. Biol. Inorg. Chem. 1*, 117−126.
40. Guiles, R. D., Sarma, S., DiGate, R. J., Banville, D., Basus, V. J., Kuntz, I. D., and Waskell, L. (1996) *Nat. Struct. Biol. 3*, 333−339.
41. Banci, L., Bertini, I., Gori Savellini, G., Romagnoli, A., Turano, P., Cremonini, M. A., Luchinat, C., and Gray, H. B. (1997) *Proteins: Struct., Funct., Genet. 29*, 68−76.
42. Banci, L., Dugad, L. B., La Mar, G. N., Keating, K. A., Luchinat, C., and Pierattelli, R. (1992) *Biophys. J. 63*, 530−543.
43. Bertini, I., Jonsson, B.-H., Luchinat, C., Pierattelli, R., and Vila, A. J. (1994) *J. Magn. Reson., Ser. B 104*, 230−239.
44. Bertini, I., Luchinat, C., Piccioli, M., Vicens Oliver, M., and Viezzoli, M. S. (1991) *Eur. Biophys. J. 20*, 269−279.
45. Blaszak, J. A., Ulrich, E. L., Markley, J. L., and McMillin, D. R. (1982) *Biochemistry 21*, 6253−6258.
46. Bertini, I., Viezzoli, M. S., Luchinat, C., Stafford, E., Cardin, A. D., Behnke, W. D., Bhattacharyya, L., and Brewer, C. (1987) *J. Biol. Chem. 262*, 16984−16994.
47. Ming, L. J., Banci, L., Luchinat, C., Bertini, I., and Valentine, J. S. (1988) *Inorg. Chem. 27*, 4458−4463.
48. Zannoni, D. (1989) *Bichim. Biophys. Acta 975*, 299.
49. Baker, E. N. (1988) *J. Mol. Biol. 203*, 1071.
50. Nar, H., Messerschmidt, A., Huber, R., van de Kamp, M., and Canters, G. W. (1991) *J. Mol. Biol. 218*, 427.
51. Nar, H., Messerschimdt, A., Huber, R., van de Kamp, M., and Canters, G. W. (1991) *J. Mol. Biol. 221*, 765−772.
52. Romero, A., Hoitink, C. W. G., Nar, H., Huber, R., Messerschmidt, A., and Canters, G. W. (1993) *J. Mol. Biol. 229*, 1007−1021.
53. Murphy, L. M. M., Strange, R. W., Karlsson, G. B., Lundberg, L. G., Pascher, T., Reinhammar, B., and Hasnain, S. (1993) *Biochemistry 32*, 1965−1975.
54. Karlson, B. G., Tsai, L. C., Nar, H., Sanders-Loehr, J., Bonander, N., Langer, V., and Sjolin, L. (1997) *Biochemistry 36*, 4089−4095.
55. Guss, J. M., and Freeman, H. C. (1983) *J. Mol. Biol. 169*, 521−563.
56. Guss, J. M., Harrowell, P. R., Murata, M., Norris, V. A., and Freeman, H. C. (1986) *J. Mol. Biol. 192*, 361−387.
57. Hart, P. J., Nersissian, A. M., Herrmann, R. G., Nalbandyan, R. M., Valentine, J. S., and Eisenberg, D. (1996) *Protein Sci. 5*, 2175−2183.
58. Kalverda, A. P., Wymenga, S. S., Lommen, A., van de Ven, F. J. M., Cees, W. H., and Canters, G. W. (1994) *J. Mol. Biol. 240*, 358−371.
59. Coremans, J. W. A., Poluektov, O. G., Groenen, E. J. J., Canters, G. W., Nar, H., and Messerschmidt, A. (1994) *J. Am. Chem. Soc. 116*, 3097−3101.
60. Salgado, J., Jimenez, H. R., Donaire, A., and Moratal, J. M. (1995) *Eur. J. Biochem. 231*, 358−369.
61. Moratal Mascarell, J. M., Salgado, J., Donaire, A., Jimenez, H. R., and Castells, J. (1993) *Inorg. Chem. 32*, 3587−3588.
62. Moratal Mascarell, J. M., Salgado, J., Donaire, A., Jimenez, H. R., Castells, J., and Martinez Ferrer, M.-J. (1993) *Magn. Reson. Chem. 31*, S41−S46.
63. Moratal Mascarell, J. M., Salgado, J., Donaire, A., Jimenez, H. R., and Castells, J. (1993) *J. Chem. Soc. , Chem. Commun.*, 110−112.
64. Salgado, J., Jimenez, H. R., Moratal, J. M., Kroes, S. J., Warmerdam, G. C. M., and Canters, G. W. (1996) *Biochemistry 35*, 1810−1819.
65. Jimenez, H. R., Salgado, J., Moratal, J. M., and Morgenstern-Badarau, I. (1996) *Inorg. Chem. 35*, 2737−2741.
66. Moratal, J. M., Romero, A., Salgado, J., Perales-Alarcon, A., and Jimenez, H. R. (1995) *Eur. J. Biochem. 228*, 653−657.
67. Bonander, N., Vanngard, T., Tsai, L. C., Langer, V., Nar, H., and Sjolin, L. (1997) *Proteins: Struct., Funct., Genet. 27*, 385−394.
68. Piccioli, M., Luchinat, C., Mizoguchi, T. J., Ramirez, B. E., Gray, H. B., and Richards, J. H. (1995) *Inorg. Chem. 34*, 737−742.

69. Parr, S. R., Barber, D., Greenwood, C., Phillips, B. W., and Melling, J. (1976) *Biochem. J. 157*, 423−430.
70. Rance, M., Sörensen, O. W., Bodenhausen, G., Wagner, G., Ernst, R. R., and Wüthrich, K. (1983) *Biochem. Biophys. Res. Commun. 117*, 479.
71. Bax, A., Griffey, R. H., and Hawkins, B. L. (1983) *J. Magn. Reson. 55*, 301−315.
72. Jeener, J., Meier, B. H., Bachmann, P., and Ernst, R. R. (1979) *J. Chem. Phys. 71*, 4546−4553.
73. Griesinger, C., Otting, G., Wüthrich, K., and Ernst, R. R. (1988) *J. Am. Chem. Soc. 110*, 7870−7872.
74. Cavanagh, J., and Rance, M. (1990) *J. Magn. Reson. 88*, 72−85.
75. Bax, A., and Davis, D. G. (1985) *J. Magn. Reson. 65*, 355−360.
76. Marion, D., and Wüthrich, K. (1983) *Biochem. Biophys. Res. Commun. 113*, 967−974.
77. van de Kamp, M., Canters, G. W., Wijmenga, S. S., Lommen, A., Hilbers, C. W., Nar, H., and Messerschmidt, A. (1992) *Biochemistry 31*, 10194−10207.
78. Oh, B.-H., and Markley, J. L. (1990) *Biochemistry 29*, 3993−4004.
79. Oh, B.-H., Mooberry, E. S., and Markley, J. L. (1990) *Biochemistry 29*, 4004−4011.
80. Oh, B.-H., and Markley, J. L. (1990) *Biochemistry 29*, 4012−4017.
81. Xia, B., Westler, W. M., Cheng, H., Meyer, J., Moulis, J.-M., and Markley, J. L. (1995) *J. Am. Chem. Soc. 117*, 5347−5350.
82. La Mar, G. N. (1973) in *NMR of Paramagnetic Molecules* (La Mar, G. N., Horrocks, W. D. W., and Holm, R. H., Eds.) Academic Press, New York.
83. Banci, L., Bertini, I., Luchinat, C., Donaire, A., Martinez, M.-J., and Moratal Mascarell, J. M. (1990) *Comments Inorg. Chem. 9*, 245−261.
84. Karplus, M. (1963) *J. Am. Chem. Soc. 85*, 2870−2871.
85. Ho, F. F.-L., and Reilley, C. N. (1969) *Anal. Chem. 41*, 1835−1841.
86. Pratt, L., and Smith, B. B. (1968) *Trans. Faraday Soc. 65*, 915−927.
87. Bertini, I., Donaire, A., Feinberg, B. A., Luchinat, C., Piccioli, M., and Yuan, H. (1995) *Eur. J. Biochem. 232*, 192−205.
88. Huber, J. G., Gaillard, J., and Moulis, J.-M. (1995) *Biochemistry 34*, 194−205.
89. Wang, P. L., Donaire, A., Zhou, Z. H., Adams, M. W. W., and La Mar, G. N. (1996) *Biochemistry 35*, 11319−11328.
90. Sheppard, S. K., Eaton, G. R., and Eaton, S. S. (1989) *Inorg. Chem. 28*, 4496−4499.
91. Eaton, D. R., Josey, A. D., Phillips, W. D., and Benson, R. E. (1962) *J. Chem. Phys. 37*, 347−360.
92. Eaton, D. R., Josey, A. D., Benson, R. E., Phillips, W. D., and Cairns, T. L. (1962) *J. Am. Chem. Soc. 84*, 4100−4106.
93. Happe, J. A., and Ward, R. L. (1963) *J. Chem. Phys. 39*, 1211−1218.
94. Kluiber, R. W., and Horrocks, W. D., Jr. (1965) *J. Am. Chem. Soc. 87*, 5350−5356.
95. Kluiber, R. W., and Horrocks, W. D., Jr. (1967) *Inorg. Chem. 6*, 166.
96. Holm, R. H., Everett, G. W., and Horrocks, W. D., Jr. (1966) *J. Am. Chem. Soc. 88*, 1071.
97. Wu, F.-J., and Kurtz, D. M., Jr. (1989) *J. Am. Chem. Soc. 111*, 6563−6572.
98. Langen, R., Jensen, G. M., Jacob, U., Stephen, P. J., and Warshel, A. (1992) *J. Biol. Chem. 267*, 25625−25627.
99. Huang, J., Ostrander, R. L., Rheingold, A. L., Leung, Y., and Walters, M. A. (1994) *J. Am. Chem. Soc. 116*, 6769−6776.
100. Moore, G. R., Pettigrew, G. W., and Rogers, N. K. (1986) *Proc. Natl. Acad. Sci. U.S.A. 83*, 4998−4999.
101. SKjeldahl, L., Westler, W. M., Oh, B.-H., Krezel, A. M., Holden, H. M., Jacobson, B. L., Rayment, I., and Markley, J. L. (1991) *Biochemistry 30*, 7363−7368.
102. Mouesca, J. M., Rius, G. J., and Lamotte, B. (1993) *J. Am. Chem. Soc. 115*, 4714−4731.
103. Rius, G. J., and Lamotte, B. (1989) *J. Am. Chem. Soc. 111*, 2464−2469.
104. Doan, P. E., Fan, C., and Hoffman, B. M. (1994) *J. Am. Chem. Soc. 116*, 1033−1041.
105. Penfield, K. W., Gay, R. R., Himmelwright, R. S., Eickman, N. C., Norris, V. A., Freeman, H. C., and Solomon, E. I. (1981) *J. Am. Chem. Soc. 103*, 4382−4388.
106. Mizoguchi, T. J., Di Bilio, A. J., Gray, H. B., and Richards, J. H. (1992) *J. Am. Chem. Soc. 114*, 10076−10078.
107. Han, J., Loehr, T. M., Valentine, J. S., Averill, B. A., and Sanders-Loehr, J. (1993) *J. Am. Chem. Soc. 115*, 4256−4263.
108. Coremans, J. W. A., Poluektov, O. G., Groenen, E. J. J., Canters, G. W., Nar, H., and Messerschmidt, A. (1997) *J. Am. Chem. Soc. 119*, 4726−4731.
109. Penfield, K. W., Gewirth, A. A., and Solomon, E. I. (1985) *J. Am. Chem. Soc. 107*, 4519−4529.
110. Salgado, J. (1995) Ph.D. Dissertation, University of Valencia, Valencia, Spain.
111. Vila, A. J. and Fernandez, C. O. (1996) *J. Am. Chem. Soc. 118*, 7291−7298.
112. Ubbink, M., Lian, L. Y., Modi, S., Evans, P. A., and Bendall, D. S. (1996) *Eur. J. Biochem. 242*, 132−147.

BI971974F